Available online at www.sciencedirect.com

SciVerse ScienceDirect

Ceramics International 39 (2013) 8073–8078

CERAMICS INTERNATIONAL

www.elsevier.com/locate/ceramint

Novel all solution processed heterojunction using p-type cupric oxide and n-type zinc oxide nanowires for solar cell applications

Ian Y.Y. Bu

Department of Microelectronics Engineering, National Kaohsiung Marine University, 81157 Nanzih District, Kaohsiung City, Taiwan, Republic of China

Received 8 March 2013; received in revised form 25 March 2013; accepted 25 March 2013
Available online 6 April 2013

Abstract

Nanostructured three-dimensional heterojunctional photovoltaic devices were synthesized through combination of hydrothermal synthesis of zinc oxide nanowires (ZnO NWs) and sol–gel derived cupric oxide. The ZnO NWs were prepared by the hydrothermal method at 90 °C, whereas the CuO thin films were synthesized by the sol–gel method. The derived CuO thin films were thoroughly characterized through scanning electron microscopy, X-ray diffraction, energy dispersive spectroscopy, UV–vis spectroscopy and electrical measurement. It was found that power conversion efficiency ~0.3% can be obtained through the proposed combination.

Keywords: Copper oxide; Zinc oxide nanowire; Heterojunction; Solution processed

1. Introduction

Recently, Zinc oxide (ZnO) nanowires have attracted great attention due to potential enhancements in various technological applications [1–3]. Noteworthy features include direct band gap (3.37 eV at room temperature), large exciton binding energy (60 meV), high transparency and inherent n-type conduction behavior [4]. Therefore, ZnO materials have been widely proposed as active materials in applications such as UV LEDs [5] and transparent conductive electrodes [6,7]. Although n-type ZnO can be easily obtained, it is quite difficult to achieve stable p-type ZnO due to the well-known dopant compensation effect [8]. Consequently, n-type ZnO is often paired with stable p-type material such as Cu_2O [9], p-$SrCu_2O_2$ [10] and CuO [11]to form pn junction for optoelectronic devices. Cupric oxide (CuO) is a p-type semiconductor with a band gap of 1.2 eV that is non-toxic and available in large abundance [12]. The properties of these semiconductor nanomaterials can be further adjusted by its size, shape and crystallinity. Previous studies have demonstrated successful synthesis of variety of ZnO based nanomaterials ranging from ZnO nanoparticles [13], nanosheets [14], nanorods [15], nanowhisker [16] and nanoribbons [17]. The obtained ZnO nanomaterials can be combined with CuO to form low-cost solar cells. Such combination provides an alternative route to fabricate all-oxide based heterojunctional devices that has desired conduction band alignment. Theoretically, the maximum power conversion efficiency predicted by Schockley–Queisser, considering only radiative recombination, for CuO based photovoltaic device is around 30%, which is significantly higher than the predicted value for its close derivative (Cu_2O) 20% [18]. Nevertheless, most of the previous studies have focused on the combination of Cu_2O/ZnO [9,19,20], whereas CuO/ZnO based heterojunctions have been relatively overlooked. Hsueh et al. [21] deposited Cu_2O coated ZnO nanowires through combination of chemical vapor process and sputtering, whereas, Kuo et al. produced ZnO:Al/CuO_2 hetreojunction via chemical vapor process and electron beam evaporation [22]. Recently, Cui et al. fabricated ZnO/CuO_2 solar cells with power conversion efficiency of around 0.88% with a combined electrochemical deposition process [23]. From a processing point of view, it would be attractive to develop a one-system fabrication process and simple equipment setup process i.e. without change of deposition method between the materials. Solution-based deposition methods are attractive due to the possibility of shape and size control without the requirement of complicated equipment. Sol–gel deposition process has been well established to synthesis of other metal oxide materials such as TiO_2 [24] and ZnO [25] and is attractive due to its simplicity, great chemical composition control, inkjet process capability and high material utilization.

E-mail address: ianbu@hotmail.com

0272-8842/$ - see front matter © 2013 Elsevier Ltd and Techna Group S.r.l. All rights reserved.
http://dx.doi.org/10.1016/j.ceramint.2013.03.079

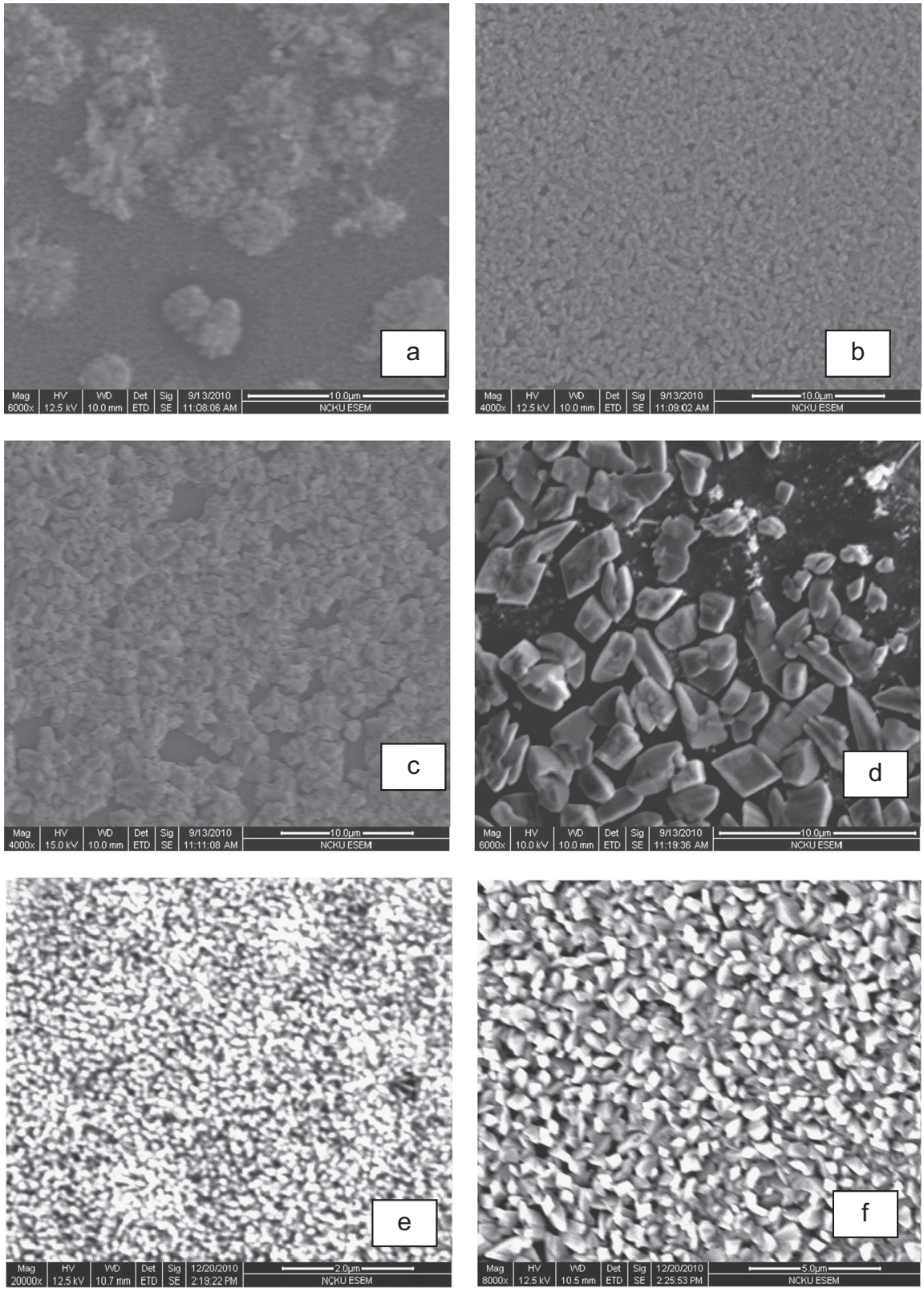

Fig. 1. Sol–gel synthesis of CuO thin films post sintered at (a) 400 °C (b) 450 °C (c) 500 °C and (d) 550 °C. (d) Shows the as deposited ZnNW and (e) shows the CuO coated ZnNW.

In this study, we report a simple solution based approach to synthesize ZnO/CuO nanostructured heterojunction. The first part of the paper discusses the optimization of CuO thin films using sol–gel deposition through scanning electron microscopy, X-ray diffraction and energy dispersive spectroscopy. Then the optimized CuO thin film was applied onto prepared

ZnO nanowire and evaluated using UV–vis spectroscopy and electrical measurements.

2. Experimental

2.1. Hydrothermal growth of ZnO nanowire

All chemicals were of reagent grade, purchased from sigma Aldrich and used without further purification. ZnO nanowire arrays were grown via two step method; seed preparation and hydrothermal nanowire growth. Specifically, ZnO seed layer was prepared by sol–gel precursor that consisted of 10 mM ethanoic solution of zinc acetate. Uniform seed layer was formed by spin coating the prepared sol at 3000 rpm and post annealing at 100 °C. Vertically aligned ZnO were then grown by immersing the seed-coated substrate into a aqueous solution of equimolar (0.0025 M) zinc nitrate hexahydrate ($Zn(NO_3)_2 \cdot 6H_2O$) and hexamethylenetetramine for 2 h.

2.2. Sol–gel CuO

Cupric chloride ($CuCl_2$) was used for preparation of CuO films with isopropanol (IPA) as the solvent. First, 0.7 M of $CuCl_2$ was dissolved in IPA by magnetically stirring at 60 °C for 2 h to yield a homogeneous solution. Corning glass substrates were cleaned in acetone, IPA and D.I. water for 10 min at each step and blown dried by N_2 gun. The solution was drop casted onto the pre-cleaned glass substrate and rotated at 3000 rpm for 30 s. After the deposition by spin coating, the film was pre-heated at 250 °C for 30 min on a hotplate to ensure complete evaporation of the solvent. Subsequently, the deposited films were post-annealed in air at 400–550 °C for 1 h.

2.3. Characterization

The film composition and surface structure of the samples were examined by using a FEI Quanta 400 F Environmental Scanning Electron Microscope (ESEM), equipped with an Energy Dispersive Spectroscopy (EDS). The structure and crystal orientation of the deposited films were measured by a Siemens D5000 X-Ray diffractometer, which uses the Cu Kα radiation. Electrical current–voltage measurements were taken by source meter (Keithley 2400). In order to ensure Ohmic contacts to the fabricated device, the front electrodes were formed by Au evaporation through metal masks defined with 60 μm diameter. Solar cell characteristics were measured using a commercially available solar simulator (Science tech) with 100 $mWcm^{-2}$ (AM 1.5 conditions).

3. Results and discussions

Fig. 1(a–d) shows the SEM images of the CuO thin film prepared on glass substrate by the sol–gel technique as a function of sintering temperature. Clearly, it can be seen that the formation of CuO is highly dependent on the calcination temperature. CuO thin films synthesized at 400 °C exhibit several large clusters of particles with average diameter of around 5 μm embedded within a film of nanoparticles. As the sintering temperature is raised to 450 °C (Fig. 1(b)), more nanoparticles nucleated and uniformally coated the glass substrate. Such trend continued as the sintering temperature increased to > 500 °C with increased nucleation and appearance of larger crystallites. It would appear that the thermal annealing step between 400 and 450 °C provides CuO crystallization, whereas annealing temperature > 550 °C provides sufficient energy for grain growth. Fig. 1(e) displays the hydrothermally grown ZnO nanowires before CuO coating. It can be observed from Fig. 1(e) that the ZnO nanowires are densely packed with strong vertical orientation to the substrate. Typically, geometry of synthesized ZnO nanowires consisted of 50 nm diameter and 5 μm in length with aspect ratio of ~10. Subsequently, CuO was deposited onto the ZnO nanowires using the sol–gel precursor at 550 °C. Fig. 1(f) top view of CuO coated ZnO NW. It can be observed that the sample still retained the appearance of nanowire arrays, but decorated with CuO on the ZnO NWs.

Structural properties of the sol–gel derived cupric oxide thin films were investigated by XRD. Fig. 2 displays the XRD spectra of the thin films sintered in air. All the synthesized films exhibit 2 dominant peak at 35.5 and 38.7° that can be assigned to (002) and (111) orientation of CuO monoclinic crystal phase. Clearly, higher annealing temperature results in enhanced diffraction peak intensity. The increase in XRD intensity can be attributed to progressive crystallization of CuO. As the sintering temperature increases to 550 °C, additional diffraction peaks appear. All the additional peaks could be indexed to monoclinic CuO (JCPDS 48-1548) at (202), (020), (202), (113), (022), (311) and (220). It is reassuring that diffraction peaks ascribed to CuO_2 and Cu_4O_3 are absent from the XRD pattern, indicating the purity of as-deposited sample. The XRD data correlated well with the previous study on sol–gel synthesis of CuO (deposited at process temperature between 360 and 550 °C) that revealed only CuO phases form above 360 °C, below this temperature the films consisted of Cu_2O [26]. It is interesting to note that films annealed at 550 °C resulted in significant enhancement in XRD peaks and crystal nucleation.

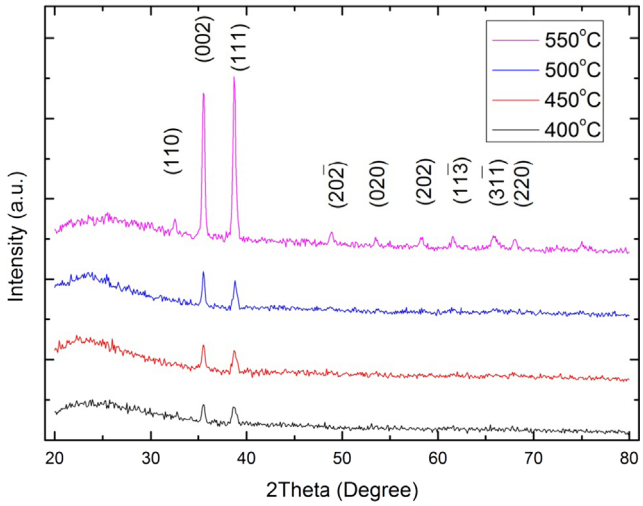

Fig. 2. XRD pattern for CuO thin films sintered at 400–550 °C.

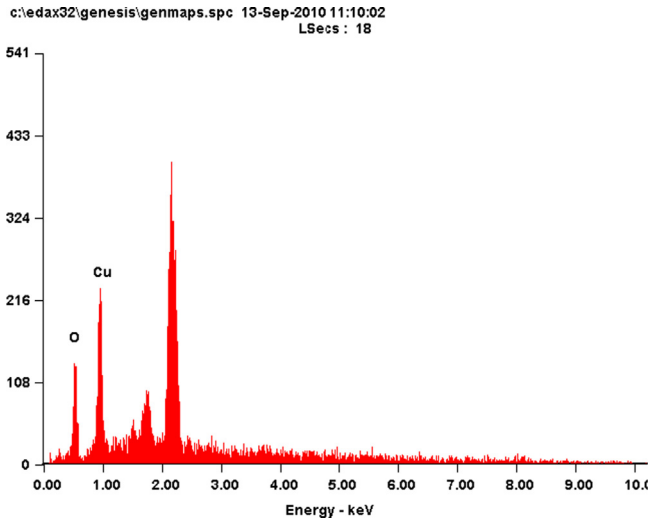

Element	Wt%	At%
OK	26.43	58.79
CuL	73.57	41.21
Matrix	Correction	ZAF

Fig. 3. Representative EDS analysis of sol–gel synthesized CuO samples.

Such trend is expected to continue as sintering temperature increases. However, sintering temperature beyond 600 °C would be close to the softening points of inexpensive substrates and prevent its usage.

In order to quantify the elemental composition of the deposited films, EDS analysis was performed on the sol–gel derived CuO samples. Fig. 3 shows the representative EDS compositional analysis of the CuO samples. The atomic ratio of copper and oxygen from the EDS spectrum is 41.21:58.79. Peaks centered at around 1.6 and 2.3 eV are from the silicon substrate and evaporated gold, respectively. These peaks were not indexed to enable evaluation of the Cu/O ratio. The as-derived CuO samples are slightly oxygen-rich probably due to interstitial oxygen.

The sol–gel synthesis of CuO was achieved through dissolving $CuCl_2$ in IPA to form copper hydroxide. Subsequently, CuO was formed through the annealing process according to the following reaction:

$$Cu^{2+} + 2(OH)^- \rightarrow Cu(OH)_2$$

$$Cu(OH)_2 \rightarrow CuO + H_2O$$

Fig. 4 shows the optical transmittance of the glass/ITO/ZnO nanowire and glass/ITO/ZnO/CuO heterojunction, respectively. Prior to p-type CuO deposition the glass/ITO/ZnO nanowire sample exhibits around 50% transparency at wavelength ~500 nm. Usually, ZnO thin films are highly transparent and have been extensively investigated as alternative to indium tin oxide as transparent conductive oxides. However, as the dimension of ZnO is reduced from micron towards nanometer scale, transparency reduces due to enhanced light scattering from the nanomaterial. Fig. 4 also shows the effect of sol–gel deposition of CuO on top of ZnO nanowire on

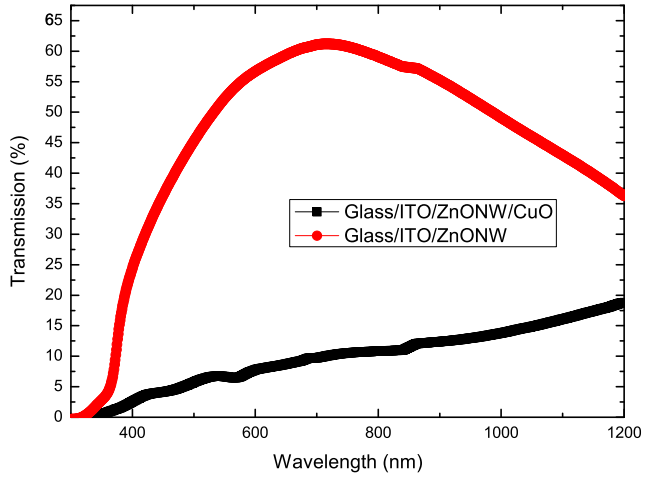

Fig. 4. Optical transmittance of glass/ITO/ZnO NW and glass/ITO/ZnO NW/CuO as determined by UV–vis.

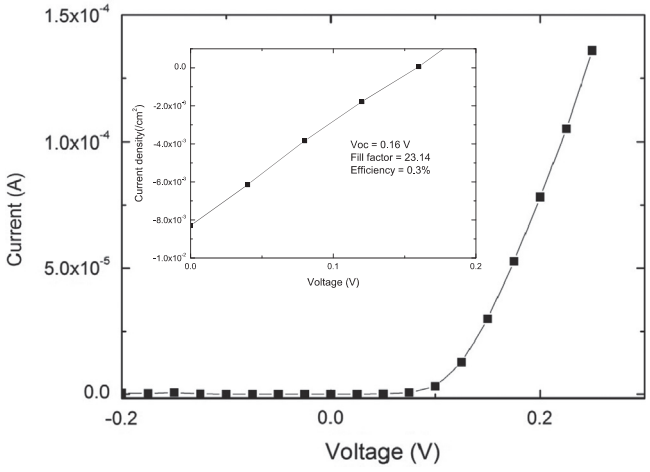

Fig. 5. Dark *IV* characteristics of the deposited ITO/ZnNW/CuO device and inset *JV* characteristics of the deposited ITO/ZnNW/CuO device.

transparency. When compared with the glass/ITO/ZnO nanowire sample, glass/ITO/ZnO/CuO heterojunction shows around 90% drop in transparency (5% at 500 nm). Since CuO posses a narrower band gap than ZnO, the majority of the photons is expected to be absorbed through CuO. This effect is further enhanced by the underneath ZnO nanowire template, which offers multiple chances of photon absorption through nanostructure enhanced surface area.

Fig. 5 shows the *I–V* characteristics measured from coaxial CuO/ZnO nanowires. From Hall measurements, it was determined that the carrier concentration of the CuO layer is ~3.234×10^{18} cm^{-3}, whereas the ZnO nanowire is n-type with carrier concentration of around 5.899×10^{17} cm^{-3}. Consequently, the p–n junction is formed between the ZnO NW and CuO.It is reassuring that the fabricated CuO/ZnO heterojunction exhibit rectifying behavior, which confirms p–n junction formation. Under forward bias condition, the CuO/ZnO heterojunction exhibits exponential increase in current at forward bias around 0.13 Vand low reverse leakage current ~1.611×10^{-7} A. Previous reports on oxide-based junctions

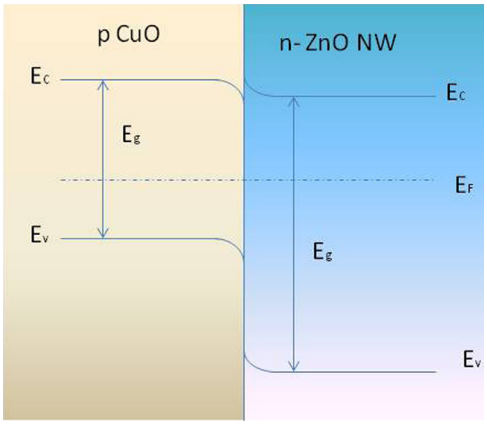

Fig. 6. Energy band diagram for the proposed heterojunction.

have cited that the electrical characteristics are sensitive towards interface defects [27]. The fabricated CuO/ZnO nanowire diode heterojunction, exhibits low reverse leakage current due to low level of interface defect recombination interface between ZnO NW and CuO. Previous studies on ZnO coated CuO nanowire showed cut in voltage of around 4 V [28]. The difference is due to the process temperature used and the order of deposition material. Jung's study used process temperature ~800 °C, which are beyond the softening point of most glass and limit scalability. Photovoltaic behavior of coaxial CuO/ZnO nanowires heterojunction device was measured under simulated solar illumination. It was found that the short current density, open voltage, fill factor and power conversion efficiency of the fabricated device were 8.23 mA/cm^2, 0.16, 23.14 and 0.3%, respectively. The low power conversion originates from the lack of connectivity between the ZnO NW and ITO layer. During the synthesis of ZnO nanowires, seed layers were prepared onto ITO substrate by spin-coating process. In order to ensure formation of nanowires rather than thin films, seed layers are not well connected, which could introduce additional resistance into the device. Although the power conversion efficiency is low, the proposed deposition process in this present study can be further optimized (materials optimization, ZnO nanowire diameter and length) and is potentially useful for ultra-low cost photovoltaic applications.

Fig. 6 illustrates a schematic energy band diagram of the ZnO–CuO pn junction under thermal equilibrium condition. The energy band gap of n-type ZnO and p-type CuO is around 3.32 eV and 1.2 eV, respectively. The band offsets of the conduction band (delta Ec) and valence band (delta Ev) are around 0.28 eV and 1.72 eV, respectively. Under illumination, hole-electron pairs are generated with the electron excited into the conduction band and holes in the valence band. As CuO possesses comparatively narrower band gap than ZnO, most of the light are expected to be absorbed by p-type CuO.

4. Conclusion

In this study, a novel solution-based process was used to fabricate CuO coated ZnO nanowires. The advantages of proposed method includes utilization of earth abundant, non-toxic material and simple-setup that can be scaled-up for large area deposition. It was found that rectified heterojunction can be formed through sol–gel deposition of CuO onto ZnO NW. Furthermore, it was found that short current density, open voltage, fill factor and power conversion efficiency of the fabricated device were 8.23 mA/cm^2, 0.16, 23.14 and 0.3%.

Acknowledgment

The author would like to thank National Science Council for financial support, under the grant code NSC 98-2218-E-022 -001 and NSC 99-2628-E-022-001.

References

[1] M. Shamsipur, S.M. Pourmortazavi, S.S. Hajimirsadeghi, M.M. Zahedi, M. Rahimi-Nasrabadi, Facile synthesis of zinc carbonate and zinc oxide nanoparticles via direct carbonation and thermal decomposition, Ceramics International (2012).
[2] I.Y. Bu, Rapid synthesis of ZnO nanostructures through microwave heating process, Ceramics International (2012).
[3] S. Musić, A. Šarić, Formation of hollow ZnO particles by simple hydrolysis of zinc acetylacetonate, Ceramics International (2012).
[4] C. Jagadish, S.J. Pearton, Zinc oxide bulk, thin films and nanostructures: processing, properties and applications, Elsevier Science, 2006.
[5] B. de Lacy Costello, R. Ewen, N.M. Ratcliffe, M. Richards, Highly sensitive room temperature sensors based on the UV–LED activation of zinc oxide nanoparticles, Sensors and Actuators B: Chemical 134 (2) (2008) 945–952.
[6] N. Talebian, M.R. Nilforoushan, Z. Salehi, Effect of heterojunction on photocatalytic properties of multilayered ZnO-based thin films, Ceramics International (2012).
[7] C. Yang, M. Hon, I. Leu, Patterned Zn-seeds and selective growth of ZnO nanowire arrays on transparent conductive substrate and their field emission characteristics, Ceramics International (2012).
[8] V. Avrutin, D.J. Silversmith, H. Morkoç, Doping asymmetry problem in ZnO: current status and outlook, Proceedings of the IEEE 98 (7) (2010) 1269–1280.
[9] S. Jeong, A. Mittiga, E. Salza, A. Masci, S. Passerini, Electrodeposited ZnO/Cu2O heterojunction solar cells, Electrochimica Acta 53 (5) (2008) 2226–2231.
[10] S. Kim, H. Seok, H. Lee, M. Lee, D. Choi, K. Chai, Fabrication of transparent p–n junction diode based on oxide semiconductors deposited by RF magnetron sputtering, Ceramics International 38 (2012) S623–S626.
[11] S. Mridha, D. Basak, Investigation of a p-CuO/n-ZnO thin film heterojunction for H2 gas-sensor applications, Semiconductor Science and Technology 21 (2006) 928.
[12] A. Rakhshani, Preparation, characteristics and photovoltaic properties of cuprous oxide—a review, Solid-state Electronics 29 (1) (1986) 7–17.
[13] H. Faber, M. Burkhardt, A. Jedaa, D. Kälblein, H. Klauk, M. Halik, Low-temperature solution-processed memory transistors based on zinc oxide nanoparticles, Advanced Materials 21 (30) (2009) 3099–3104.
[14] U. Maiti, K. Chattopadhyay, S. Karan, B. Mallik, Synthesis of a zinc oxide nanosheet–nanowire network complex by a low-temperature chemical route: Efficient UV detection and field emission property, Scripta Materialia 62 (5) (2010) 305–308.
[15] I.Y.Y. Bu, Rapid synthesis of ZnO nanostructures through microwave heating process, Ceramics International (2012).
[16] D.W. Wang, M.S. Cao, J. Yuan, H.B. Lin, Q.L. Zhao, D.Q. Zhang, Fabrication, microstructure and properties of zinc oxide nanowhisker reinforced lead zirconate titanate nanocomposites, Current Nanoscience 7 (2) (2011) 227–234.

[17] A.R. Botello-Méndez, F. López-Urías, M. Terrones, H. Terrones, Magnetic behavior in zinc oxide zigzag nanoribbons, Nano Letters 8 (6) (2008) 1562–1565.
[18] A. Mittiga, E. Salza, F. Sarto, M. Tucci, R. Vasanthi, Heterojunction solar cell with 2% efficiency based on a Cu_2O substrate, Applied Physics Letters 88 (16) (2006).
[19] M. Izaki, T. Shinagawa, K.T. Mizuno, Y. Ida, M. Inaba, A. Tasaka, Electrochemically constructed p-Cu_2O/n-ZnO heterojunction diode for photovoltaic device, Journal of Physics D: Applied Physics 40 (2007) 3326.
[20] J. Katayama, K. Ito, M. Matsuoka, J. Tamaki, Performance of Cu_2O/ZnO solar cell prepared by two-step electrodeposition, Journal of Applied Electrochemistry 34 (7) (2004) 687–692.
[21] T.J. Hsueh, C.L. Hsu, S.J. Chang, P.W. Guo, J.H. Hsieh, I. Chen, Cu_2O/n-ZnO nanowire solar cells on ZnO: Ga/glass templates, Scripta Materialia 57 (1) (2007) 53–56.
[22] C.L. Kuo, R.C. Wang, J.L. Huang, C.P. Liu, C.K. Wang, S.P. Chang, W. H. Chu, C.H. Wang, C. Tu, The synthesis and electrical characterization of Cu_2O/Al: ZnO radial p–n junction nanowire arrays, Nanotechnology 20 (2009) 365603.
[23] Y. Cui, C. Wang, G. Liu, H. Yang, S. Wu, T. Wang, Fabrication and photocatalytic property of ZnO nanorod arrays on Cu_2O thin film, Materials Letters (2011).
[24] A. Testino, I.R. Bellobono, V. Buscaglia, C. Canevali, M. D'Arienzo, S. Polizzi, R. Scotti, F. Morazzoni, Optimizing the photocatalytic properties of hydrothermal TiO_2 by the control of phase composition and particle morphology. A systematic approach, Journal of the American Chemical Society 129 (12) (2007) 3564–3575.
[25] I.Y.Y. Bu, Facile synthesis of highly oriented p-type aluminum co-doped zinc oxide film with aqua ammonia, Journal of Alloys and Compounds 509 (6) (2011) 2874–2878.
[26] S.C. Ray, Preparation of copper oxide thin film by the sol–gel-like dip technique and study of their structural and optical properties, Solar Energy Materials & Solar Cells 68 (3) (2001) 307–312.
[27] M. Izaki, T. Shinagawa, K.-T. Mizuno, Y. Ida, M. Inaba, A. Tasaka, Electrochemically constructed p-Cu_2O/n-ZnO heterojunction diode for photovoltaic device, Journal of Physics D: Applied Physics 40 (11) (2007) 3326.
[28] S. Jung, S. Jeon, K. Yong, Fabrication and characterization of flower-like CuO–ZnO heterostructure nanowire arrays by photochemical deposition, Nanotechnology 22 (2011) 015606.